LA-UR-11-11873
Approved for public release; distribution is unlimited.

Title: SATURATED-UNSATURATED FLOW IN A COMPRESSIBLE LEAKY-UNCONFINED AQ

Author(s): Mishra, Phoolendra K.
Kuhlman, Kristopher L.
Vesselinov, Velimir V.

Intended for: DOE
Advances in Water Resources
Groundwater
Reading Room
RCRA

SATURATED-UNSATURATED FLOW IN A COMPRESSIBLE LEAKY-UNCONFINED AQUIFER

Phoolendra K. Mishra[1], Velimir V. Vessilinov[1], Kristopher L. Kuhlman[2]

[1]Hydrology, Geochemistry and Geology Group
Los Alamos National Laboratory, MS T003,
Los Alamos, NM 87545

[2]Repository Performance Department
Sandia National Laboratories, MS-1395,
Carlsbad, NM 88220

ABSTRACT

An analytical solution is developed for three-dimensional flow towards a partially penetrating large-diameter well in an unconfined aquifer bounded below by an aquitard of finite or semi-infinite extent. The analytical solution is derived using Laplace and Hankel transforms, then inverted numerically. Existing solutions for flow in leaky unconfined aquifers neglect the unsaturated zone following an assumption of instantaneous drainage assumption due to *Neuman* [1972]. We extend the theory of leakage in unconfined aquifers by (1) including water flow and storage in the unsaturated zone above the water table, and (2) allowing the finite-diameter pumping well to partially penetrate the aquifer. The investigation of model-predicted results shows that leakage from an underlying aquitard leads to significant departure from the unconfined solution without leakage. The investigation of dimensionless time-drawdown relationships shows that the aquitard drawdown also depends on unsaturated zone properties and the pumping-well wellbore storage effects.

INTRODUCTION

The assumption that the water flow and storage in the unsaturated zone is insignificant for unconfined aquifer tests was first questioned by *Nawankor et al.* [1984] and later by *Akindunni and Gillham* [1992] based upon analysis of data collected during pumping tests in Borden, Ontario Canada. Analyzing the collected tensiometer data and soil moisture measurements, the authors concluded that the proper inclusion of unsaturated zone in analytical models used for pumping test analysis would lead to improved estimates of aquifer specific yield. Several analytical solutions were developed for flow to a pumping well in an unconfined aquifer, taking into account the unsaturated zone [*Mathias and Butler* 2006, *Tartakvosky and Neuman* 2007, *Mishra and Neuman* 2010]. These models consider the unsaturated zone effects by coupling the governing flow equations at the water table; the saturated zone governed by the diffusion equation and the vadose zone governed by the linearized unsaturated zone Richards' equation, using the linearization of *Kroszynski and Dagan* [1975]. These models considered the limiting case where the pumping well has zero radius. For detailed discussion regarding the fundamental differences between these three models readers are directed to *Mishra and Neuman* [2010].

Drawdown due to pumping a large-diameter (e.g., water supply) well in an unconfined aquifer is affected by wellbore storage (*Papadopulous and Cooper*, 1967). *Narasimhan and Zhu* [1993] used a numerical model to demonstrate that early time drawdown in an unconfined aquifer tends to be dominated by wellbore storage effects. *Mishra and Neuman* [2011] developed an analytical unconfined solution, which considers both pumping-well wellbore storage capacity, and three-dimensional axi-symmetrical unsaturated zone flow. They represented unsaturated zone constitutive properties using exponential models, which result in governing equations that are mathematically tractable, while being sufficiently flexible to be fit to other widely used constitutive models like G*ardner* [1958], *Russo* [1988], *Brooks and Corey* [1964], *van Genuchten* [1980], and *Mualem* [1976]. However, *Mishra and Neuman* [2011] considered the unconfined aquifer to be resting on an impermeable boundary and therefore did not account for the potential effects of leakage from an underlying formation (e.g., an aquitard or fractured bedrock).

The classical theory of leakage for confined aquifers was originally developed by *Hantush and Jacob* [1955] assuming steady-state vertical flow in overlying and underlying aquitards and horizontal flow in the pumped aquifer. *Hantush* [1960] later modified the theory of confined leaky aquifers to include transient vertical aquitard flow, giving asymptotic expressions for early and late times. *Neuman and Witherspoon* [1969a,b] developed a more complete analytical solution for the more general multiple aquifer flow problem, but did not consider general three-dimensional aquitard flow.

Yotov [1968] first investigated the effect of leakage from underlying strata on flow in an unconfined aquifer. He adopted the *Boulton* [1954] type model to simulate unconfined aquifer flow and considered only vertical flow in aquitard. *Ehlig and Halepaska* [1976] investigated leaky-unconfined flow through a finite-difference simulation, which coupled the *Boulton* [1954] and *Hantush and Jacob* [1955] models to simulate leakage across the aquifer-aquitard boundary. *Zlotnik and Zhan* [2005] developed an analytical solution for the flow towards a fully penetrating zero-radius well in a coupled unconfined aquifer–aquitard system where both the unsaturated zone and the horizontal aquitard flow are neglected. *Zhan and Bian* [2006] extended the work of *Zlotnik and Zhan* [2005] and developed analytical and semi-analytical methods for computing the leakage rate and water volume induced by pumping based on the works of *Hantush and Jacob*, [1955] and *Butler and Tsou* [2003]. Following *Zlotnik and Zhan* [2005], *Zhan and Bian* [2006] also neglect horizontal aquitard flow. The assumption of strictly vertical aquitard flow was justified for limiting aquifer/aquitard hydraulic conductivity contrasts by *Neuman and Witherspoon* [1969b]. Additionally, both *Zlotnik and Zhan*, [2005] and *Zhan and Bian* [2006] restrict their solutions to the case of an aquitard of semi-infinite vertical extent. *Malama et al*. [2007] developed a solution for three-dimensional aquitard flow in a finite thickness aquitard, but considered the zero-radius pumping well to be fully penetrating and ignored the flow in unsaturated zone. Here, we develop a more general leaky-unconfined aquifer solution by considering a partially penetrating large-diameter well and including the effects of unsaturated zone flow following *Mishra and Neuman* [2011]. The solution is used to investigate the effect of an aquitard on drawdown in overlying unconfined aquifer. We conclude by investigating the effects of wellbore storage capacity and the unsaturated zone on drawdown observed in the aquitard.

LEAKY-UNCONFINED THEORY

Statement of Problem

We consider a compressible unconfined aquifer of infinite radial extent resting on a finitely thick aquitard (Figure 1). The aquifer and aquitard are each spatially uniform, homogeneous and anisotropic, with constant specific storage S_s and S_{s_1}, respectively (a subscript 1 indicates aquitard-related properties). The aquifer has a fixed anisotropy ratio $K_D = K_z / K_r$ of vertical K_z to horizontal K_r saturated hydraulic conductivity. The aquitard vertical and horizontal hydraulic conductivities are K_{z_1} and K_{r_1}. The aquifer is fully saturated beneath an initially horizontal water table at elevation $z = b$ defined as the $\psi = 0$ isobar where ψ is pressure head. A saturated capillary fringe at non-positive pressure $\psi_a \le \psi \le 0$ extends from the water table to the $\psi = \psi_a$ isobar; $\psi_a \le 0$ is the pressure head required for air to enter a saturated medium. Prior to the onset of pumping the saturated hydraulic system (aquifer and aquitard) is at uniform initial hydraulic head $h_0 = b + \psi_a$. Starting at time $t = 0$, water is pumped at a constant volumetric flowrate Q from a well with finite radius r_w and wellbore storage coefficient C_w (volume of water released from storage in the pumping well per unit drawdown in the well casing). The pumping well penetrates the saturated zone between depths l and d below the initial water table. Under these conditions the drawdown $s(r,z,t) = h(r,z,0) - h(r,z,t)$ in the saturated zone is governed by the diffusion equation

$$K_r \frac{1}{r}\frac{\partial}{\partial r}\left(r\frac{\partial s}{\partial r}\right)+K_z\frac{\partial^2 s}{\partial z^2}=S_s\frac{\partial s}{\partial t} \qquad r \ge r_w \qquad 0 \le z < b, \tag{1}$$

along with the far-field boundary condition

$$s(\infty,z,t)=0, \tag{2}$$

the no-flow condition at the portion of the well casing that is not open to the aquifer

$$\left(r\frac{\partial s}{\partial r}\right)_{r=r_w}=0 \qquad 0 \le z \le b-l \qquad b-d \le z \le b, \tag{3}$$

and the wellbore storage mass-balance expression

$$2\pi K_r(l-d)\left(r\frac{\partial s}{\partial r}\right)_{r=r_w}-C_w\left(\frac{\partial s}{\partial t}\right)_{r=r_w}=-Q \qquad b-l \le z \le b-d. \tag{4}$$

The corresponding linearized unsaturated water flow equations (*Mishra and Neuman,* 2010) are

$$K_r k_0(z)\frac{1}{r}\frac{\partial}{\partial r}\left(r\frac{\partial \sigma}{\partial r}\right)+K_z\frac{\partial}{\partial z}\left(k_0(z)\frac{\partial \sigma}{\partial z}\right)=C_0(z)\frac{\partial \sigma}{\partial t} \qquad r \ge r_w \qquad b < z < b+L, \tag{5}$$

where $\sigma(r,z,t)$ is drawdown in the unsaturated zone, $k_0(z)$ is relative permeability and $C_0(z)$ is moisture capacity (slope of the curve representing water saturation as a function of pressure head) functions with the functional dependence limitations on the respective constitutive models

$$k_0(z)=k(\theta_0) \qquad C_0(z)=C(\theta_0), \tag{6}$$

the initial condition

$$\sigma(r,z,0)=0, \tag{7}$$

the far-field boundary condition

$$\sigma(\infty,z,t)=0, \tag{8}$$

the no-flow condition at the ground surface

$$\left.\frac{\partial \sigma}{\partial z}\right|_{z=b+L} = 0 \qquad r \ge r_w \tag{9}$$

and the no-flow condition at the well casing

$$\left(r\frac{\partial \sigma}{\partial r}\right)_{r=0} = 0 \qquad b < z < b+L. \tag{10}$$

The interface conditions providing continuity across the water table are

$$s - \sigma = 0 \qquad r \ge r_w \qquad z = b, \tag{11}$$

$$\frac{\partial s}{\partial z} - \frac{\partial \sigma}{\partial z} = 0 \qquad r \ge r_w \qquad z = b. \tag{12}$$

Aquitard drawdown $s_1(r,z,t)$ is governed by

$$K_{r_1}\frac{1}{r}\frac{\partial}{\partial r}\left(r\frac{\partial s_1}{\partial r}\right) + K_{z_1}\frac{\partial^2 s_1}{\partial z^2} = S_{s_1}\frac{\partial s_1}{\partial t} \qquad r \ge 0 \qquad -b_1 \le z < 0. \tag{13}$$

Additionally, aquitard flow satisfies no-flow conditions at the bottom and center of the flow system

$$\left. r\frac{\partial s_1}{\partial r}\right|_{r_w} = \left.\frac{\partial s_1}{\partial z}\right|_{z=-b_1} = 0. \tag{14}$$

The interface condition across the aquifer-aquitard boundary is

$$s - s_1 = 0 \qquad r \ge r_w \qquad z = 0 \tag{15}$$

$$K_z\frac{\partial s}{\partial z} = K_{z_1}\frac{\partial s_1}{\partial z} \qquad r \ge r_w \qquad z = 0. \tag{16}$$

Like *Mishra and Neuman* [2010], we represent the aquifer moisture retention curve using an exponential function

$$S_e = \frac{\theta(\psi) - \theta_r}{S_y} = e^{a_c(\psi - \psi_a)} \qquad a_c \ge 0 \qquad \psi_a \ge 0 \tag{17}$$

where S_e is effective saturation, θ_r is residual water content and $S_y = \theta_s - \theta_r$ is drainable porosity or specific yield. We also adopt the *Gardner* [1958] exponential model for relative hydraulic conductivity,

$$k(\psi) = \begin{cases} e^{a_k(\psi - \psi_k)} & \psi \le \psi_k \\ 1 & \psi < \psi_k \end{cases} \qquad a_k \ge 0 \qquad \psi_k \ge 0, \tag{18}$$

with parameters a_k and ψ_k that generally differ from a_c and ψ_a in (17). The parameter ψ_k represents a pressure head above which relative hydraulic conductivity is effectively unity, which is sometimes but not always is the air-entry pressure head ψ_a. In addition to rendering the resulting equations mathematically tractable, these exponential constitutive models are sufficiently flexible to provide acceptable fits to standard constitutive models such as those mentioned earlier.

Point Drawdown in Saturated and Unsaturated Zones of the Unconfined Aquifer and Aquitard

Following *Mishra and Neuman* [2011], it is shown in Appendix A that drawdown in the saturated zone can be decomposed as

$$s = s_C + s_U \tag{19}$$

where s_C is solution for flow to a partially penetrating well of finite radius in a confined aquifer and s_U is a solution accounting for the underlying aquitard, water table, and unsaturated zone effects. The Laplace transformed solution $\overline{s}_C$ is given by *Mishra and Neuman* [2011] as

$$\bar{s}_C\left(r_D,z_D,p_D\right)=\frac{Q}{4\pi T p_D}C_0\,\mathrm{K}_0\left(r_D\phi_0\right)+\sum_{n=1}^{\infty}C_n\,\mathrm{K}_0\left(r_D\phi_n\right)\cos\left[n\pi\left(1-z_D\right)\right] \tag{20}$$

where

$$C_0=\frac{2}{\Omega(0)},\ C_n=\frac{\left[\sin\left(n\pi l_D\right)\text{-}\sin\left(n\pi d_D\right)\right]}{\pi^2\left(l_D-d_d\right)n\Omega(n)},\ \Omega(n)=r_{wD}\phi_0\,\mathrm{K}_1\left(r_{wD}\phi_n\right)+\frac{C_{wD}}{2\left(l_D-d_D\right)}r_{wD}^2\phi_n^2\,\mathrm{K}_0\left(r_{wD}\phi_n\right),$$

$r_{wD}=r_w/r$, $r_D=r/b$, $z_D=z/b$, $d_D=d/b$, $l_D=l/b$, $p_D=pt$, $C_{wD}=C_w/\left(\pi S_s b r_w^2\right)$, p is the Laplace parameter, $\phi_n=\sqrt{p_D/t_s+r_D^2K_Dn^2\pi^2}$, and K_0 and K_1 are second-kind modified Bessel functions of orders zero and one.

The Laplace transformed unsaturated zone drawdown $\bar{\sigma}$ is given by *Mishra and Neuman* [2011] and is presented in Appendix D for sake of completeness.

The Laplace transformed $\bar{s}_U$ derived in Appendix B is

$$\bar{s}_U(r_D,z_D,p_D)=\int_0^{\infty}\left\{\rho_1e^{\mu z_D}+\rho_2e^{-\mu z_D}\right\}\frac{r_D^2K_D}{r^2}y\,\mathrm{J}_0\left[yK_D^{1/2}r_D\right]\mathrm{dy} \tag{21}$$

where $\rho_1=\dfrac{\left(\dfrac{\mu}{qb}+1\right)e^{-\mu}\left(\bar{\bar{s}}_C\right)_{z_D=0}-\left(\dfrac{\mu}{q_1b}+1\right)\left(\bar{\bar{s}}_C\right)_{z_D=1}}{\Delta}$, $\rho_2=\dfrac{\left(\dfrac{\mu}{qb}-1\right)e^{\mu}\left(\bar{\bar{s}}_C\right)_{z_D=0}-\left(\dfrac{\mu}{q_1b}-1\right)\left(\bar{\bar{s}}_C\right)_{z_D=1}}{\Delta}$,

$q_1b=R_{K_z}\mu_1\tanh\left(\mu_1R_b\right)$, $\mu_1^2=\dfrac{y^2}{R_{K_D}}+\dfrac{p_D}{t_sK_Dr_D^2R_{K_D}R_{\alpha_s}}$, $R_{K_D}=\dfrac{K_{D_1}}{K_D}$, $R_{K_z}=\dfrac{K_{z_1}}{K_z}$, $R_{\alpha_s}=\dfrac{\alpha_{s_1}}{\alpha_s}$, $R_b=\dfrac{b_1}{b}$,

$\alpha_{s_1}=K_{r_1}/S_{s_1}$ and $\Delta=\left(\dfrac{\mu}{qb}+1\right)\left(\dfrac{\mu}{q_1b}-1\right)e^{-\mu}-\left(\dfrac{\mu}{qb}-1\right)\left(\dfrac{\mu}{q_1b}+1\right)e^{\mu}$.

The Laplace transformed aquitard drawdown derived in Appendix C is

$$\overline{s}_1(r_D,z_D,p_D)=\int_0^\infty \frac{\left(\overline{\overline{s}}_C\right)_{z_D=0}+\rho_1+\rho_2}{\cosh\left(\mu_1 b_1/b\right)}\ \cosh\left[\mu_1\left(z_D+R_b\right)\right]\frac{r_D^2 K_D}{r^2}\,y\,\mathrm{J}_0\left[yK_D^{1/2}r_D\right]\mathrm{dy} \tag{22}$$

where $\left(\overline{\overline{s}}_C\right)_{z_D}$ is the Laplace-Hankel transformed confined aquifer drawdown and is defined in Appendix D.

The time domain equivalents s_C, s_U, s_1 and σ of $\overline{s}_C$, $\overline{s}_U$ and $\overline{\sigma}$ are obtained through numerical Laplace transform inversion using the algorithm of *de Hoog et al.* [1982].

Vertically Averaged Observation Well Drawdown

Drawdown in an observation well that penetrates the saturated zone between elevations $z_{D1}=z_1/b$ and $z_{D2}=z_2/b$ (Figure 1) is obtained by averaging the point drawdown over this interval according to

$$s_{z_{D2}-z_{D1}}(r_D,t_s)=\frac{1}{z_{D2}-z_{D1}}\int_{z_{D1}}^{z_{D2}} s^*\left(r_D,z_D,t_s\right)dz_D \tag{23}$$

where s^* can be either aquifer drawdown *s*, aquitard drawdown s_1, or a combination of the two, depending on the observation well screen interval.

Delayed Piezometer or Observation Well Response

When water level is measured in a piezometer or observation well having storage coefficient *C* the water level observed in the borehole is delayed in time. Following *Mishra and Neuman* [2011], the measured (delayed) drawdown s_m can be expresses in terms of formation drawdown s via

$$s_m = s\left[1 - e^{-t/t_B}\right] \tag{24}$$

where t_B is basic (characteristic) monitoring well time lag. The dimensionless equivalent of (24) is

$$s_{mD} = s_D\left[1 - e^{-t_s/t_{Bs}}\right] \tag{25}$$

where $t_{Bs} = \frac{\alpha_s t_B}{r^2}$, and r is the radial distance to the monitoring location.

MODEL-PREDICTED DRAWDOWN BEHAVIOR

We illustrate the impacts of an underlying aquitard on unconfined aquifer drawdown for the case where $K_D = 1$, $S_s b / S_y = 10^{-3}$, $a_{kD} = a_{cD} = 10$, $\psi_{aD} = \psi_{kD}$, $d_D = 0.0$, $C_{wD} = 10^3$, $l_D = 0.6$ and $r_w / b = 0.02$, where $a_{kD} = a_k b$, $a_{cD} = a_c b$, $\psi_{aD} = \psi_a / b$, and $\psi_{kD} = \psi_k / b$. We also investigate the effects that wellbore storage capacity of the pumping well, the unconfined aquifer, and the unsaturated zone have on aquitard drawdown.

Dimensionless unconfined aquifer time-drawdown

We start by considering drawdown at two locations in the unconfined aquifer saturated zone, one location closer to water table ($z_D = 0.75$) and the other closer to the aquitard-aquifer boundary ($z_D = 0.25$). Figures 2a and 2b compare variations in dimensionless drawdown $s_D\left(r_D, z_D, t_s\right) = \left(4\pi K_r b / Q\right) s\left(r_D, z_D, t_s\right)$ with dimensionless time $t_s = \alpha_s t / r^2$ at $z_D = 0.25$ and $z_D = 0.75$ predicted by our proposed solution and the solutions of *Mishra and Neuman* [2011], *Neuman* [1972], and the modified solution of *Malama et al.* [2007] (modified to include the partially penetrating pumping well effects, as done in *Malama et al.* [2008] for a multi-aquifer system). The solutions of *Neuman* [1972] and *Malama et al*. [2007] do not include wellbore storage effects, and therefore they overestimate drawdown at early time. Both of these solutions also ignore the unsaturated zone above the water table, considering the water table a material boundary. Our proposed solution follows *Mishra and Neuman* [2011] when leakage effects are minor, but our solution predicts less drawdown when leakage effects are significant. It is seen in Figure 2b that solution of *Mishra and Neuman* [2011] overestimates drawdown near the aquitard at intermediate time because it does not include aquitard leakage. Near the water table (Figure 2a) the effects of aquitard leakage are minimal and our proposed solution approaches *Mishra and Neuman* [2011] at all times.

Figures 3a and 3b show dimensionless time-drawdown variations at dimensionless radial distance $r_D = 0.5$ and dimensionless unconfined aquifer saturated zone elevation $z_D = 0.25$ with different values of $R_{K_z} = K_{z_1} / K_z$ when the radial aquitard hydraulic conductivity is large ($R_{K_r} = 1$) and small ($R_{K_r} = 1.0 \times 10^{-6}$). When the radial hydraulic conductivity in aquitard is negligible ($R_{K_r} = 1.0 \times 10^{-6}$), aquitard flow is predominately vertical; larger values of vertical aquitard hydraulic conductivity cause decreases in intermediate time drawdown (Figure 3a). It is seen from Figure 3b that when aquitard horizontal hydraulic conductivity is large ($R_{K_r} = 0.1$) the amount drawdown is reduced from further increases in aquitard vertical hydraulic conductivity also extend to the later time.

Figure 4 depicts the effect of $R_{K_r} = K_{r_1} / K_r$ on the dimensionless time-drawdown at dimensionless radial distance $r_D = 0.5$ and dimensionless unconfined aquifer saturated zone elevation $z_D = 0.25$ when $R_{K_z} = 0.1$. Radial flow in the aquitard results in less drawdown at late time than that predicted by *Mishra and Neuman* [2011], who do not account for aquitard leakage.

Figure 5 presents the effect of hydraulic conductivity of an isotropic aquitard on dimensionless time-drawdown at dimensionless radial distance $r_D = 0.5$ and dimensionless unconfined aquifer saturated zone elevation $z_D = 0.25$. When aquitard hydraulic conductivity is less than two orders of magnitude smaller than the unconfined aquifer, the effects of leakage on the aquifer drawdown are negligible. This is in agreement with findings of *Neuman and Witherspoon* [1969b] for confined aquifers. They found errors <5% attributable to the vertical aquitard flow assumption, when the hydraulic conductivity contrast between the aquifer and aquitard was at least two orders of magnitude. Figure 5 also presents a case where the hydraulic conductivity of the zone underlying unconfined aquifer is larger than the aquifer. Because the proposed model accounts for general three-dimensional flow in underlying zone, we can consider the case where the lower layer is more permeable than the aquifer ($R_{K_r} = 2$).

Figure 6 shows how the dimensionless unconfined aquifer time-drawdown is affected by aquitard thickness. When the aquitard thickness is less than the initial unconfined aquifer saturated thickness ($R_b \leq 1$) aquitard leakage only affects the time-drawdown curve at intermediate time. Figure 6 shows that further increases in aquitard thickness beyond eight times the initial unconfined aquifer saturated zone thickness have negligible effect on the time-drawdown curve.

Dimensionless aquitard time-drawdown

Figure 7 depicts dimensionless aquitard drawdown $s_D\left(r_D, z_D, t_s\right) = \left(4\pi K_r b / Q\right) s_1\left(r_D, z_D, t_s\right)$ variations with dimensionless time $t_s = \alpha_s t / r^2$ at dimensionless radial distance $r_D = 0.2$ and dimensionless aquitard elevation $z_D = -0.25$ for different values of C_{wD}. As with solution of *Mishra and Neuman* [2011] for non-leaky systems, aquitard drawdown is impacted by pumping-well wellbore storage capacity. Larger wellbore storage factors impact the aquitard drawdown for a longer period.

Figure 8 depicts the effect that changes in a_{kD}, the dimensionless relative hydraulic conductivity exponent, have on dimensionless time-drawdown at dimensionless radial distance $r_D = 0.2$ and dimensionless aquitard elevation $z_D = -0.25$. For larger values of a_{kD}, the hydraulic conductivity of the unsaturated zone decreases at a faster rate as pressure drops (becomes more negative) relative to its threshold (ψ_k). The rate water drains under a given hydraulic gradient from the unsaturated zone into the saturated zone diminishes, decreasing dimensionless aquitard drawdown. For very large a_{kD}, unsaturated hydraulic conductivity drops precipitously as pressure head falls below ψ_k, causing the unsaturated zone to be effectively impermeable.

We conclude this analysis by showing in Figure 9 the effects that changes in a_{cD}, the dimensionless effective saturation exponent, have on dimensionless time-drawdown at dimensionless radial distance $r_D = 0.2$ and dimensionless aquitard elevation $z_D = -0.25$. When both exponents are large, hydraulic conductivity and pressure head in the unsaturated zone drop (the latter becoming negative) quickly as pressure head approaches the thresholds ψ_k and ψ_c. The unsaturated zone loses its ability to store water above the water table, causing this surface to behave as a moving boundary, which leads to the limiting-case behavior of instantaneous drainage due to *Neuman* [1972]. Consequently, for large values of exponents (Figure 9, red curve) our solution reduces to that the solution of *Malama et al*. [2007], which relies on the assumption of instantaneous drainage of *Neuman* [1972]. As a_{cD} decreases, the capacity of the unsaturated zone to store water at a given negative pressure head increases, causing delayed water table response to diminish and dimensionless drawdown to increase earlier than predicted by *Malama et al*. [2007].

CONCLUSIONS

Our work leads to the following major conclusions:

1. A new analytical solution was developed for axially symmetric saturated-unsaturated three dimensional radial flow to a well with wellbore storage that partially penetrates the saturated zone of a compressible vertically anisotropic leaky-unconfined aquifer. The solution accounts for both radial and vertical flow in the unsaturated zone and the underlying aquitard.

2. Because the solution considers three-dimensional radial flow in the aquitard, any properties may be assigned to the aquitard, allowing the solution to also be used to simulate leakage from underlying bedrock or other non-aquitard layers (e.g., an unscreened aquifer region with different hydraulic properties).

3. Aquitard leakage can lead to significant departures from solutions that do not account for leakage, e.g., *Mishra and Neuman* [2011]. However, the effect of leakage on unconfined aquifer drawdown diminishes at points farther away from the aquifer-aquitard boundary.

4. Unsaturated zone effects are often more important than leakage effects when the observation location is close to the water table.

5. For large diameter pumping wells, at early time water is withdrawn entirely from the wellbore storage. Solution that do not account for wellbore storage predict a much larger early rise in drawdown.

6. Aquitard drawdown is also affected by the pumping-well wellbore storage capacity. As in the unconfined aquifer, larger wellbore storage capacity leads to larger impacts on the observed aquitard drawdown.

7. The unsaturated zone properties not only affect the unconfined aquifer time-drawdown behavior but they also impact the observed aquitard response.

APPENDIX A: DECOMPOSITION OF SATURATED ZONE SOLUTION

In a manner analogous to *Mishra and Neuman* [2010] we decompose s into two parts

$$s = s_C + s_U \tag{A1}$$

where s_C is solution for a partially penetrating well in a confined aquifer, satisfying

$$\frac{1}{r}\frac{\partial}{\partial r}\left(r\frac{\partial s_C}{\partial r}\right) + K_D\frac{\partial^2 s_C}{\partial z^2} = \frac{1}{\alpha_s}\frac{\partial s_C}{\partial t} \qquad r \geq r_w \qquad 0 \leq z < b \tag{A2}$$

$$s_C(r,z,0) = 0 \qquad r \geq r_w \tag{A3}$$

$$s_C(\infty,z,t) = 0 \tag{A4}$$

$$\left.\frac{\partial s_C}{\partial z}\right|_{z=\{0,b\}} = 0 \qquad r \geq r_w \tag{A5}$$

$$\left(\frac{\partial s_C}{\partial r}\right)_{r=r_w} = 0 \qquad 0 \leq z \leq b-l \qquad b-d \leq z \leq b \tag{A6}$$

$$2\pi K_r(l-d)\left(\frac{\partial s_C}{\partial r}\right)_{r=r_w} - C_W\left(\frac{\partial s_C}{\partial t}\right)_{r=r_w} = -Q \qquad b-l \leq z \leq b-d\,. \tag{A7}$$

and s_U is a solution that takes into account aquitard and saturated-unsaturated unconfined conditions, but has no pumping source term, satisfying

$$\frac{1}{r}\frac{\partial}{\partial r}\left(r\frac{\partial s_U}{\partial r}\right) + K_D\frac{\partial^2 s_U}{\partial z^2} = \frac{1}{\alpha_s}\frac{\partial s_U}{\partial t} \qquad r \geq r_w \qquad 0 \leq z < b \tag{A8}$$

$$s_U(r,z,0) = 0 \qquad r \geq r_w \tag{A9}$$

$$s_U(\infty,z,t) = 0 \tag{A10}$$

$$\frac{\partial s_U}{\partial z} - \frac{K_{z_1}}{K_z}\frac{\partial s_1}{\partial \text{z}} = 0 \qquad r \geq r_w \qquad z = 0 \tag{A11}$$

$$\left(\frac{\partial s_U}{\partial r}\right)_{r=r_w} = 0 \qquad\qquad 0 \le z \le b \qquad\qquad \text{(A12)}$$

subject to interface conditions at the water table,

$$s_C + s_U - \sigma = 0 \qquad\qquad r \ge r_w \qquad\qquad z = b \qquad\qquad \text{(A13)}$$

$$\frac{\partial s_C}{\partial z} + \frac{\partial s_U}{\partial z} - \frac{\partial \sigma}{\partial z} = 0 \qquad\qquad r \ge r_w \qquad\qquad z = b. \qquad\qquad \text{(A14)}$$

APPENDIX B: LAPLACE SPACE SOLUTION FOR SATURATED ZONE

Equations (A1) – (A14) are solved by sequential application of the finite cosine transform, the Hankel transform,

$$f(a) = \int_0^\infty r\,\mathrm{J}_o(ar)\,f(r)\,dr \qquad\qquad \text{(B1)}$$

and Laplace transform

$$f(p) = \int_0^\infty f(t)e^{-pt}dt \qquad\qquad \text{(B2)}$$

with Hankel parameter a and Laplace parameter p, J_0 being zero-order first-kind Bessel function.

Mishra and Neuman [2011] showed that the transform of the confined aquifer solution is

$$\begin{aligned}\bar{\bar{s}}_C\left(a, z_D, p_D\right) = {} & C_0\left\{\frac{r_w}{a}\mathrm{J}_1\left(ar_w\right)\mathrm{K}_0\left(r_w\tau_0\right) + \frac{\tau_0 r_w \mathrm{J}_0\left(ar\right)\mathrm{K}_1\left(r\tau_0\right) - ar_w\mathrm{J}_1\left(ar\right)\mathrm{K}_0\left(r\tau_0\right)}{a^2+\tau_0^2}\right\} \\ & + \sum_{n=1}^{\infty} C_n\left\{\frac{r_w}{a}\mathrm{J}_1\left(ar_w\right)\mathrm{K}_0\left(r_w\tau_0\right) + \frac{\tau_n r_w \mathrm{J}_0\left(ar\right)\mathrm{K}_1\left(r\tau_n\right) - ar_w\mathrm{J}_1\left(ar\right)\mathrm{K}_0\left(r\tau_n\right)}{a^2+\tau_n^2}\right\}\cos\left[n\pi\left(1-z_D\right)\right]\end{aligned} \qquad \text{(B3)}$$

where $\eta^2 = a^2/K_D + p/\alpha_s K_D$.

The Laplace transform of (A8)–(A14) is

$$\frac{1}{r}\frac{\partial}{\partial r}\left(r\frac{\partial \bar{s}_U}{\partial r}\right)+K_D\frac{\partial^2 \bar{s}_U}{\partial z^2}=\frac{p}{\alpha_s}\bar{s}_U \qquad 0\le z<b \qquad \text{(B4)}$$

$$\bar{s}_U\left(\infty,z,p\right)=0 \qquad \text{(B5)}$$

$$\left.\frac{\partial \bar{s}_U}{\partial z}\right|_{z=0}=0 \qquad \text{(B6)}$$

$$\left.r\frac{\partial \bar{s}_U}{\partial r}\right|_{r_w}=0 \qquad 0\le z\le b \qquad \text{(B7)}$$

$$\bar{s}_C+\bar{s}_U-\bar{\sigma}=0 \qquad z=b \qquad \text{(B8)}$$

$$\frac{\partial \bar{s}_C}{\partial z}+\frac{\partial \bar{s}_U}{\partial z}-\frac{\partial \bar{\sigma}}{\partial z}=0 \qquad z=b. \qquad \text{(B9)}$$

Taking the Hankel transform of (B4) – (B9) yields

$$-a^2\bar{\bar{s}}_U+K_D\frac{\partial^2 \bar{\bar{s}}_U}{\partial z^2}=\frac{p}{\alpha_s}\bar{\bar{s}}_U \qquad 0\le z<b \qquad \text{(B10)}$$

$$\bar{\bar{s}}_C+\bar{\bar{s}}_U-\bar{\bar{\sigma}}=0 \qquad z=b \qquad \text{(B11)}$$

$$\frac{\partial \bar{\bar{s}}_U}{\partial z}-\frac{\partial \bar{\bar{\sigma}}}{\partial z}=0 \qquad z=b \qquad \text{(B12)}$$

$$\frac{\partial \bar{\bar{s}}_U}{\partial z}-\frac{K_{z_1}}{K_z}\frac{\partial \bar{\bar{s}}_1}{\partial z}=0 \qquad z=0. \qquad \text{(B13)}$$

The general solution of (B10) subject to (B11) is

$$\bar{\bar{s}}_U=\rho_1e^{\eta z}+\rho_2e^{-\eta z}. \qquad \text{(B14)}$$

Consider that $\left(\partial\bar{\bar{s}}_C/\partial z\right)=0$ at $z=0$ and $z=b$ by virtue of (A5), along with

$$\frac{\partial \bar{\bar{\sigma}}}{\partial z}=q\left(\bar{\bar{s}}_C+\bar{\bar{s}}_U\right) \qquad z=b \qquad \text{(B15)}$$

together with q, which is derived in (D15) of *Mishra and Neuman* [2011],

$$\frac{\partial \bar{\bar{s}}_U}{\partial z} = q_1\left(\bar{\bar{s}}_C + \bar{\bar{s}}_U\right) \qquad z = 0 \tag{B16}$$

together with q_1 , which is derived in (C7), we obtain from (B12)–(B14)

$$\rho_1 = \frac{q_1\left(\eta+q\right)e^{-\eta b}\left(\bar{\bar{s}}_C\right)_{z=0} - q\left(\eta+q_1\right)\left(\bar{\bar{s}}_C\right)_{z=b}}{\Delta}, \tag{B17}$$

$$\rho_2 = \frac{q_1\left(\eta-q\right)e^{\eta b}\left(\bar{\bar{s}}_C\right)_{z=0} - q\left(\eta-q_1\right)\left(\bar{\bar{s}}_C\right)_{z=b}}{\Delta}, \tag{B18}$$

where $\Delta = \left(\eta-q_1\right)\left(\eta+q\right)e^{-\eta b} - \left(\eta-q\right)\left(\eta+q_1\right)e^{\eta b}$.

According to *Mishra and Neuman* [2011], the Lapalce–Hankel transformed drawdown in confined aquifer can be written as

$$\begin{aligned}\bar{\bar{s}}_C\left(a, z_D, p_D\right) = {} & C_0\left\{\frac{r_w}{a}\mathrm{J}_1\left(ar_w\right)\mathrm{K}_0\left(r_w\tau_0\right) + \frac{\tau_0 r_w \mathrm{J}_0\left(ar\right)\mathrm{K}_1\left(r\tau_0\right) - ar_w\mathrm{J}_1\left(ar\right)\mathrm{K}_0\left(r\tau_0\right)}{a^2+\tau_0^2}\right\} \\ & + \sum_{n=1}^{\infty} C_n\left\{\frac{r_w}{a}\mathrm{J}_1\left(ar_w\right)\mathrm{K}_0\left(r_w\tau_0\right) + \frac{\tau_n r_w \mathrm{J}_0\left(ar\right)\mathrm{K}_1\left(r\tau_n\right) - ar_w\mathrm{J}_1\left(ar\right)\mathrm{K}_0\left(r\tau_n\right)}{a^2+\tau_n^2}\right\}\cos\left[n\pi\left(1-z_D\right)\right]\end{aligned}. \tag{B19}$$

The inverse Hankel transform of (B14) is

$$\bar{s}_U = \int_0^{\infty}\left\{\rho_1 e^{\eta z} + \rho_2 e^{-\eta z}\right\} a\,\mathrm{J}_0\left(ar\right)da. \tag{B20}$$

Defining a new variable $y = ar / K_D^{1/2} r_D$ transforms (B20) into the result presented in (21).

It is noted that when $q_1 = 0$ the aquiard is replaced by an impermeable boundary, and $\rho_1 = \rho_2 = \dfrac{2\left(\bar{\bar{s}}_C\right)_{z=b}}{\cosh(\eta b) - \dfrac{\eta}{q}\sinh(\eta b)}$. These simplifications reduce (B20) to equation (3) of *Mishra and Neuman* [2011].

APPENDIX C: AQUITARD SOLUTION

The Laplace–Hankel transform of the confined aquitard equations is

$$-a^2\bar{\bar{s}}_1 + K_{D1}\frac{\partial^2\bar{\bar{s}}_1}{\partial z^2} = p\frac{S_{s1}}{K_{r1}}\bar{\bar{s}}_1 \qquad -b_1 \le z < 0 . \tag{C1}$$

By virtue of the no-flow boundary condition at the bottom of the system, $\left.\frac{\partial\bar{\bar{s}}_1}{\partial z}\right|_{z=-b_1} = 0$, the general solution to (C1) is

$$\bar{\bar{s}}_1 = \rho_1\cosh\left[\eta_1\left(z+b_1\right)\right] \tag{C2}$$

where $\eta_1 = \frac{a^2}{K_{D_1}} + \frac{pS_{s_1}}{K_{r_1}K_{D_1}}$.

The boundary conditions

$$\bar{\bar{s}}_1 = \bar{\bar{s}} = \bar{\bar{s}}_C + \bar{\bar{s}}_U \qquad z = 0 \tag{C3}$$

gives

$$\bar{\bar{s}}_1 = \frac{\left(\bar{\bar{s}}_C + \bar{\bar{s}}_U\right)_{z=0}}{\cosh\left(\eta b_1\right)}\cosh\left[\eta_1\left(z+b_1\right)\right] . \tag{C4}$$

The inverse Hankel transform of (C4) is

$$\bar{s}_1 = \int_0^\infty \frac{\left(\bar{\bar{s}}_C + \bar{\bar{s}}_U\right)_{z=0}}{\cosh\left(\eta b_1\right)}\cosh\left[\eta_1\left(z+b_1\right)\right] a\,\mathrm{J}_0\left(ar\right)da . \tag{C5}$$

Defining a new variable $y = ar / K_D^{1/2} r_D$ and using (B14) transforms (C5) into the solution presented in (22).

The derivative of (C4) is

$$\frac{d\bar{\bar{s}}_1}{dz} = \eta_1 \tanh\left(\eta_1 b_1\right)\left(\bar{\bar{s}}_C + \bar{\bar{s}}_U\right) \qquad z = 0. \tag{C6}$$

The flux boundary condition at the aquifer-aquitard interface

$$\frac{\partial \bar{\bar{s}}_1}{\partial z} = \frac{K_z}{K_{z_1}} \frac{\partial \bar{\bar{s}}}{\partial z} \qquad z = 0 \tag{C7}$$

combined with (C6) gives

$$\frac{\partial \bar{\bar{s}}}{\partial z} = q_1\left(\bar{\bar{s}}_C + \bar{\bar{s}}_U\right) \qquad z = 0 \tag{C8}$$

Where $q_1 = \frac{K_{z_1}}{K_z} \eta_1 \tanh\left(\eta_1 b_1\right)$.

APPENDIX D: LAPLACE TRANSFORMED UNSATURATED ZONE DRAWDOWN

The Laplace transformed drawdown $\bar{\sigma}$ in the unsaturated zone is given by *Mishra and Neuman* [2011] as

$$\bar{\sigma}(r_D, z_{D,} p_D) = \begin{cases} -\int_0^\infty \zeta e^{a_{kD}\left(z_D - 1\right)/2} \frac{\mathrm{J}_\nu[i\phi(z_D - 1)] + \chi \mathrm{Y}_\nu[i\phi(z_D - 1)]}{\mathrm{J}_\nu[i\phi(0)] + \chi \mathrm{Y}_\nu[i\phi(0)]} \left(\bar{\bar{s}}_C\right)_{z_D = 1} \frac{r_D^2 K_D}{r^2} y \mathrm{J}_0\left(y K_D^{1/2} r_D\right) \mathrm{dy} \\ \text{for } a_{cD} \neq a_{kD} \\ -\int_0^\infty \xi \frac{e^{\delta_{1D}\left(z_D - 1\right)} + \chi e^{\delta_{2D}\left(z_D - 1\right)}}{1 + \chi} \left(\bar{\bar{s}}_C\right)_{z_D = 1} \frac{r_D^2 K_D}{r^2} y \mathrm{J}_0\left(y K_D^{1/2} r_D\right) \mathrm{dy} \\ \text{for } a_{cD} = a_{kD} = \kappa_D \end{cases} \tag{D1}$$

where $r_D = r / b$, $z_D = z / b$, $\mu^2 = y^2 + \frac{p_D}{t_s K_D r_D^2}$, $t_s = \alpha_s t / r^2$, $\alpha_s = K_r / S_s$, $q_D = qb$, $a_{kD} = a_k b$,

$a_{cD} = a_c b$, $\phi(z_D) = \sqrt{\frac{4 B_D}{\lambda_D^2} e^{\lambda_D z_D / 2}}$, $\lambda_D = a_{kD} - a_{cD}$, $B_D = p_D \frac{S_D a_{cD} e^{a_{kD}\left(\psi_{kD} - \psi_{aD}\right)}}{t_s K_D r_D^2}$, $S_D = S_y / S$,

$\psi_{kD} = \psi_k / b$, $\psi_{aD} = \psi_a / b$, $\delta_{1D,2D} = \delta_{1,2} b = \dfrac{\kappa_D \mp \sqrt{\kappa_D^2 + 4\left(B_D + y^2\right)}}{2}$, $\nu = \sqrt{\dfrac{a_{kD}^2 + 4y^2}{\lambda_D^2}}$, and $\zeta = 1 - \cosh(\mu) / \left(\cosh(\mu) - \dfrac{\mu}{q_D}\sinh(\mu)\right)$ are dimensionless quantities. The Laplace-Hankel transforms of the confined solution (B20) is

$$\left(\bar{\bar{s}}_C\right)_{z_D} = C_0 \frac{r^2}{K_D r_D^2}\left\{\frac{y_D r_{wD}}{y^2} \mathrm{J}_1\left(y_D r_{wD}\right)\mathrm{K}_0\left(r_{wD}\phi_0\right) + \frac{\Gamma(0)}{\mu^2}\right\} + \sum_{n=1}^{\infty} C_n \frac{r^2}{K_D r_D^2}\left\{\frac{y_D r_{wD}}{y^2}\mathrm{J}_1\left(y_D r_{wD}\right)\mathrm{K}_0\left(r_{wD}\phi_0\right) + \frac{\Gamma(n)}{\mu^2 + n^2\pi^2}\right\}\cos\left\{n\pi(1 - z_D)\right\}$$

(D2)

where $\Gamma(n) = r_{wD}\phi_n \mathrm{J}_0\left(y_D\right)\mathrm{K}_1\left(\phi_n\right) - y_D r_{wD}\mathrm{J}_1\left(y_D\right)\mathrm{K}_0\left(\phi_n\right)$, $y_D = y K_D^{1/2} r_D$, and J_0 and J_1 are modified Bessel functions of first kind of order zero and one. Finally, the

$$\chi = \begin{cases} -\dfrac{\left(a_{kD} + n\lambda_D\right)\mathrm{J}_n\left[i\phi\left(L_D\right)\right] - 2i\sqrt{B_D e^{\lambda_D L_D}}\,\mathrm{J}_{n+1}\left[i\phi\left(L_D\right)\right]}{\left(a_{kD} + n\lambda_D\right)\mathrm{Y}_n\left[i\phi\left(L_D\right)\right] - 2i\sqrt{B_D e^{\lambda_D L_D}}\,\mathrm{Y}_{n+1}\left[i\phi\left(L_D\right)\right]} & a_{kD} \neq a_{cD} \\ i & a_{kD} \neq a_{cD}, L_D \to \infty \\ -\dfrac{\delta_{1D}}{\delta_{2D}} e^{\left(\delta_{1D} - \delta_{2D}\right)L_D} & a_{kD} = a_{cD} \\ 0 & a_{kD} = a_{cD}, L_D \to \infty \end{cases} \quad \text{(D3)}$$

$$q_D = \begin{cases} \left(\dfrac{a_{kD}}{2} + \dfrac{n\lambda_D}{2}\right) - i\sqrt{B_D}\,\dfrac{\mathrm{J}_{n+1}\left[i\phi\left(0\right)\right] + \chi\,\mathrm{Y}_{n+1}\left[i\phi\left(0\right)\right]}{\mathrm{J}_n\left[i\phi\left(0\right)\right] + \chi\,\mathrm{Y}_n\left[i\phi\left(0\right)\right]} & a_{kD} \neq a_{cD} \\ \dfrac{\delta_{1D} + \chi\delta_{2D}}{1 + \chi} & a_{kD} = a_{cD} \\ \delta_{1D} & a_{kD} = a_{cD}, L_D \to \infty \end{cases} \quad \text{(D4)}$$

where $L_D = L/b$, J_n and Y_n are first and second kind Bessel functions of order n.

ACKNOWLEDGEMENTS

This research was partially funded by the Environmental Programs Directorate of the Los Alamos National Laboratory. Los Alamos National Laboratory is a multi-program laboratory managed and operated by Los Alamos National Security (LANS) Inc. for the U.S. Department of Energy's National Nuclear Security Administration under contract DE-AC52-06NA25396. Sandia National Laboratories is a multi-program laboratory managed and operated by Sandia Corporation, a wholly owned subsidiary of Lockheed Martin Corporation, for the U.S. Department of Energy's National Nuclear Security Administration under contract DE-AC04-94AL85000.

REFERENCES

Akindunni, F.F. and Gillham, R.W. (1992), Unsaturated and Saturated Flow in Response to pumping of an Unconfined Aquifer: Numerical Investigation of Delayed Drainage. *Ground Water*, 30(5): 690–700.

Boulton, N.S. (1954), The drawdown of the water-table under non-steady conditions near a pumped well in an unconfined formation. *Proceedings - Institution of Civil Engineers*, 3(4), 564-575.

Brooks, R.H. and A.T. Corey (1964), Hydraulic properties of porous media, *Hydrology Papers* 30, Colo. State Univ., Fort Collins.

Butler, Jr. J.J. and M.S. Tsou (2003), Pumping-induced leakage in a bounded aquifer: an example of a scale-invariant phenomenon. *Water Resources Research*, 39(12), 1344.

de Hoog, F.R., J.H. Knight, and A.N. Stokes (1982), An improved method for numerical inversion of Laplace transforms, *SIAM Journal on Scientific and Statatistical Computing*, *3*, 357–366.

Ehlig, C. and J.C. Halepaska (1976), A numerical study of confined–unconfined aquifers including effects of delayed yield and leakage. *Water Resources Research*, 12(6), 1175–1183.

Gardner, W.R. (1958), Some steady state solutions of unsaturated moisture flow equations with application to evaporation from a water table. *Soil Science*, 85(4), 228–232.

Hantush, M.S. (1960), Modification of the theory of leaky aquifers. *Journal of Geophysical Research*, 65(11), 3713–3726.

Hantush, M.S. and C.E. Jacob (1955), Nonsteady radial flow in an infinite leaky aquifer. *Eos Transactions, AGU*, 36(1), 95–100.

Kroszynski, U.I. and G. Dagan (1975), Well pumping in unconfined aquifers: the influence of the unsaturated zone, Water Resources Research, 11(3), 479-490.

Malama, B., K.L. Kuhlman and W. Barrash (2007), Semi-analytical solution for flow in leaky unconfined aquifer-aquitard systems, *Journal of Hydrology*, 346(1-2), 59–68.

Malama, B., K.L. Kuhlman and W. Barrash (2008), Semi-analytical solution for flow in a leaky unconfined aquifer toward a partially penetrating pumping well, *Journal of Hydrology*, 356(1-2), 234–244.

Mathias and Butler (2006), Linearized Richards' equation approach to pumping test analysis in compressible aquifers, *Water Resources Research,* 42, W06408.

Mishra, P.K., and S.P. Neuman (2010), Improved forward and inverse analyses of saturated-unsaturated flow toward a well in a compressible unconfined aquifer, *Water Resources Research*, 46(7), W07508.

Mishra, P.K., and S.P. Neuman (2011), Saturated-unsaturated flow to a well with storage in a compressible unconfined aquifer, *Water Resources Research*, 47(5), W05553.

Mualem, Y. (1976), A new model for predicting the hydraulic conductivity of unsaturated porous media. *Water Resources Research,* 12(3), 513–522.

Narasimhan, T. N., and M. Zhu (1993), Transient flow of water to a well in an unconfined aquifer: Applicability of some conceptual models, *Water Resources Research*, 29(1), 179–191.

Neuman, S.P. (1972), Theory of flow in unconfined aquifers considering delayed response of the water table, *Water Resources Research*, 8(4), 1031-1045.

Neuman, S.P. and P.A. Witherspoon, (1969a), Applicability of current theories to flow in leaky aquifers. *Water Resources Research*, 5(4), 817–829.

Neuman, S.P. and P.A.Witherspoon, (1969b), Theory of flow in a confined two aquifer system. *Water Resources Research*, 5(3), 803–816.

Nwankwor, G.I., J.A. Cherry, and R.W. Gillham (1984), A comparative study of specific yield determination for a shallow sand aquifer, *Ground Water*, 22(3), 303–312.

Papadopulos, I.S., and H.H. Cooper Jr. (1967), Drawdown in a well of large diameter, *Water Resources Research*, 3(1), 241–244.

Russo, D. (1988), Determining soil hydraulic properties by parameter estimation: On the selection of a model for the hydraulic properties, *Water Resources Research*, 24(3), 453–459.

Tartakovsky, G.D., and S.P. Neuman (2007), Three-dimensional saturated-unsaturated flow with axial symmetry to a partially penetrating well in a compressible unconfined aquifer, *Water Resources Research*, 43(1), W01410.

van Genuchten, M. T. (1980), A closed-form equation for predicting the hydraulic conductivity of unsaturated soils, *Soil Science Socciety of America Journal*, 44(5), 892–898.

Yang, S.-Y., H.-D. Yeh, and P.-Y. Chiu (2006), A closed form solution for constant flux pumping in a well under partial penetration condition, *Water Resources Research*, 42(5), W05502.

Yotov I.G. (1968), On drawdown around wells in leaky water table aquifer. *Comptes rendu de Academie Bulgara des Sciences*, 21(8), 765-768.

Zlotnik, V.A. and H. Zhan (2005), Aquitard effect on drawdown in water table aquifers. *Water Resources Research*, 41, W06022.

Zhan, H. and A. Bian (2006), A method of calculating pumping induced leakage. *Journal of Hydrology*, 328(3–4), 659–667.

Nomenclature Table

S_s	aquifer specific storage	L^{-1}
S_y	aquifer drainable porosity or specific yield	
S_e	effective saturation	
θ_r	residual volumetric water content	
θ_s	saturated volumetric water content	
K_r	aquifer radial hydraulic conductivity	LT^{-1}
K_z	aquifer vertical hydraulic conductivity	LT^{-1}
S_{s1}	aquitard specific storage	L^{-1}
K_{r1}	aquitard radial hydraulic conductivity	LT^{-1}
K_{z1}	aquitard vertical hydraulic conductivity	LT^{-1}
r	radial distance from the center of pumping well	L
z	vertical distance from the bottom of the aquifer (positive up)	L
t	time since pumping began	T
b	saturated thickness of unconfined aquifer before pumping begins	L
b_1	thickness of aquitard	L
l	distance from bottom of screened interval to top of aquifer	L
L	thickness of vadose zone before pumping begins	L
d	distance from top of screened interval to top of aquifer	L
r_w	diameter of pumping well	L
ψ	pressure head (less than zero when unsaturated)	L
h	hydraulic head (sum of pressure and elevation heads)	L
s	drawdown in aquifer; change in hydraulic head since pumping began	L
s_1	drawdown in aquitard; change in hydraulic head since pumping began	L
σ	drawdown in unsaturated zone; change in hydraulic head since pumping began	L
ψ_a	air-entry pressure	L
ψ_k	pressure for saturated hydraulic conductivity	L
a_c	exponent in moisture retention curve or sorptive number	L^{-1}
a_k	exponent in Gardner relative hydraulic conductivity model	L^{-1}
a	Hankel transform parameter	L^{-1}
p	Laplace transform parameter	T^{-1}
n	finite cosine transform parameter	

FIGURE CAPTIONS

Figure 1: Schematic representation of leaky unconfined aquifer-aquitard system geometry with finite radius pumping well.

Figure 2: Dimensionless leaky-unconfined aquifer drawdown versus dimensionless time at $r_D = 0.5$ when $K_D = 1$, $S_s b / S_y = 10^{-3}$, $a_{kD} = a_{cD} = 10$, $\psi_{aD} = \psi_{kD}$, $d_D = 0.0$, $l_D = 0.6$, $C_{wD} = 10^2$, $R_{K_r} = R_{K_z} = 10^{-2}$, $R_{S_s} = 10^2$, $R_b \to \infty$ and (a) $z_D = 0.75$ (b) $z_D = 0.25$. Also shown are solutions of *Mishra and Neuman* [2011], modified *Malama et al*. [2007] and *Neuman* [1972].

Figure 3: Dimensionless leaky-unconfined aquifer drawdown versus dimensionless time at $r_D = 0.5$ and $z_D = 0.75$ for $K_D = 1$, $S_s b / S_y = 10^{-3}$, $a_{kD} = a_{cD} = 10$, $\psi_{aD} = \psi_{kD}$, $d_D = 0.0$, $l_D = 0.6$, $C_{wD} = 10^2$, $R_{S_s} = 10^2$, $R_b \to \infty$ when R_{K_z} varies and (a) $R_{K_r} = 1.0 \times 10^{-6}$ (b) $R_{K_r} = 1.0$. Also shown is solution of *Mishra and Neuman* [2011].

Figure 4: Dimensionless leaky-unconfined aquifer drawdown versus dimensionless time at $r_D = 0.5$ and $z_D = 0.75$ for $K_D = 1$, $S_s b / S_y = 10^{-3}$, $a_{kD} = a_{cD} = 10$, $\psi_{aD} = \psi_{kD}$, $d_D = 0.0$, $l_D = 0.6$, $C_{wD} = 10^2$, $R_{S_s} = 10^2$, $R_{K_z} = 0.1$ and $R_b \to \infty$ when R_{K_r} varies. Also shown is solution of *Mishra and Neuman* [2011].

Figure 5: Dimensionless leaky-unconfined aquifer drawdown versus dimensionless time at $r_D = 0.5$ and $z_D = 0.75$ for $K_D = 1$, $S_s b / S_y = 10^{-3}$, $a_{kD} = a_{cD} = 10$, $\psi_{aD} = \psi_{kD}$, $d_D = 0.0$, $l_D = 0.6$, $C_{wD} = 10^2$, $R_b \to \infty$ when $R_{K_r} = R_{K_z}$ varies and $R_{S_s} = 1.0$. Also shown is solution of *Mishra and Neuman* [2011].

Figure 6: Dimensionless leaky-unconfined aquifer drawdown versus dimensionless time at $r_D = 0.5$ and $z_D = 0.75$ for $K_D = 1$, $S_s b / S_y = 10^{-3}$, $a_{kD} = a_{cD} = 10$, $\psi_{aD} = \psi_{kD}$, $d_D = 0.0$, $l_D = 0.6$, $C_{wD} = 10^2$, $R_{S_s} = 100$, $R_{K_r} = R_{K_z} = 10^{-2}$ when $R_b = b_1 / b$ varies. Also shown is solution of *Mishra and Neuman* [2011].

Figure 7: Dimensionless aquitard drawdown versus dimensionless time at $r_D = 0.5$ and $z_D = -0.25$ for $K_D = 1$, $S_s b / S_y = 10^{-3}$, $a_{kD} = a_{cD} = 10$, $\psi_{aD} = \psi_{kD}$, $d_D = 0.0$, $l_D = 0.6$, $R_{S_s} = 100$, $R_{K_r} = R_{K_z} = 10^{-2}$ when C_{wD} the dimensionless wellbore storage varies.

Figure 8: Dimensionless aquitard drawdown versus dimensionless time at $r_D = 0.5$ and $z_D = -0.25$ for $K_D = 1$, $S_s b / S_y = 10^{-3}$, $\psi_{aD} = \psi_{kD}$, $C_{wD} = 10^2$, $d_D = 0.0$, $l_D = 0.6$, $R_{S_s} = 100$, $R_{K_r} = R_{K_z} = 10^{-2}$ when $a_{cD} = 1$ and a_{kD} varies.

Figure 9: Dimensionless aquitard drawdown versus dimensionless time at $r_D = 0.5$ and $z_D = -0.25$ for $K_D = 1$, $S_s b / S_y = 10^{-3}$, $\psi_{aD} = \psi_{kD}$, $C_{wD} = 10^2$, $d_D = 0.0$, $l_D = 0.6$, $R_{S_s} = 100$, $R_{K_r} = R_{K_z} = 10^{-2}$ when $a_{kD} = 10^3$ and a_{cD} varies.

FIGURES

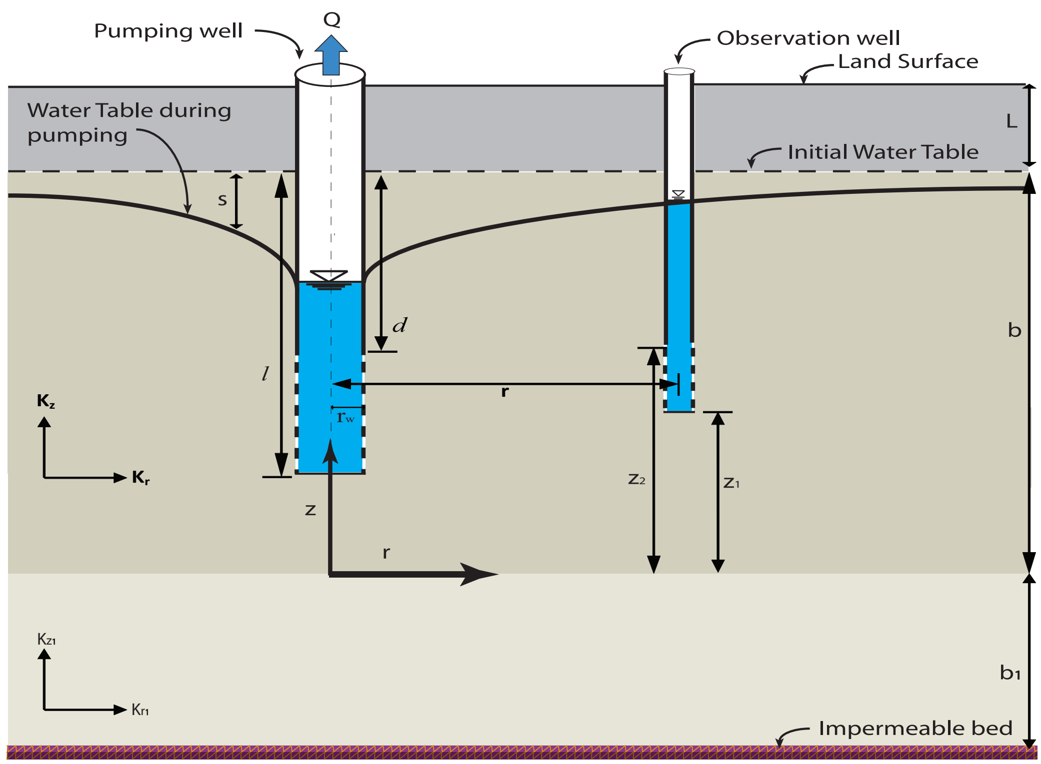

Figure 1

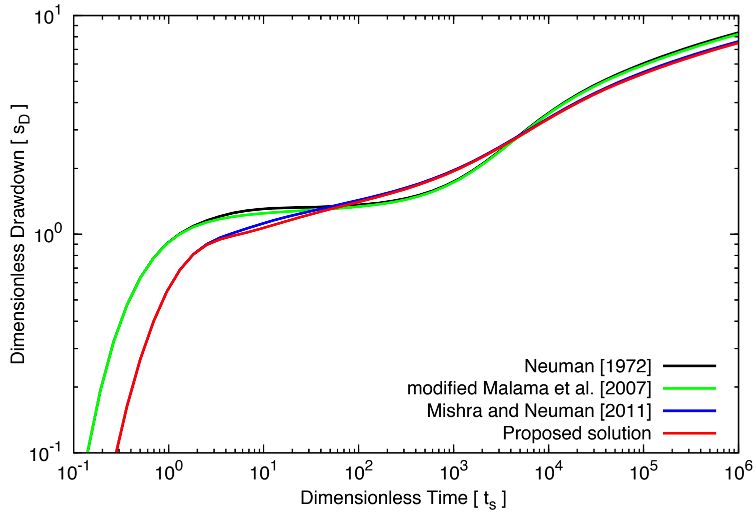

10^1
10^0
10^-1
Dimensionless Drawdown [s_D]
10^-1
10^0
10^1
10^2
10^3
10^4
10^5
10^6
Dimensionless Time [t_s]
Neuman [1972]
modified Malama et al. [2007]
Mishra and Neuman [2011]
Proposed solution

a)

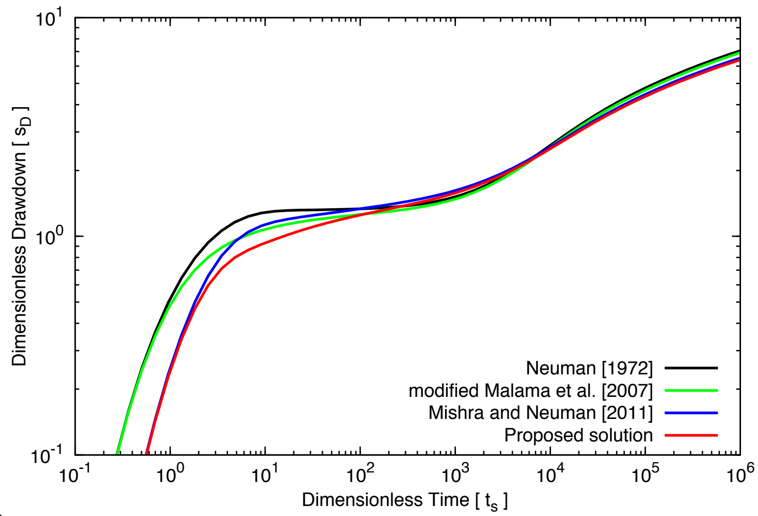

10^1
10^0
10^-1
Dimensionless Drawdown [s_D]
10^-1
10^0
10^1
10^2
10^3
10^4
10^5
10^6
Dimensionless Time [t_s]
Neuman [1972]
modified Malama et al. [2007]
Mishra and Neuman [2011]
Proposed solution

b)

Figure 2

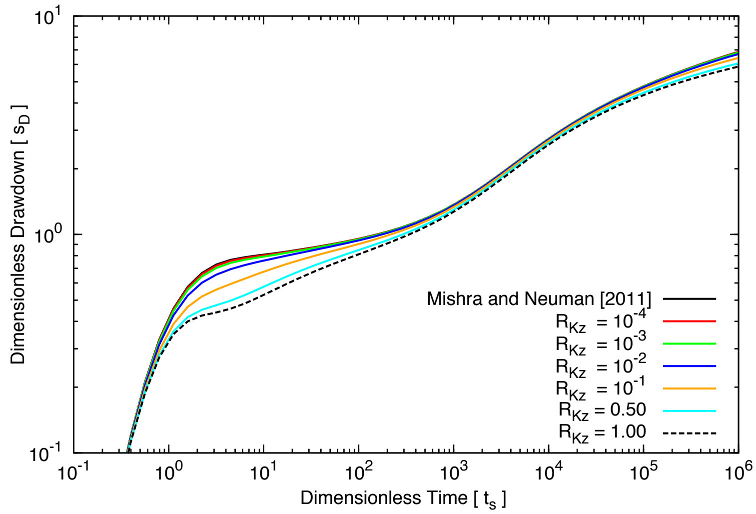
Dimensionless Drawdown [s_D]
Dimensionless Time [t_s]
10^{-1}
10^{0}
10^{1}
10^{2}
10^{3}
10^{4}
10^{5}
10^{6}
Mishra and Neuman [2011]
$R_{Kz} = 10^{-4}$
$R_{Kz} = 10^{-3}$
$R_{Kz} = 10^{-2}$
$R_{Kz} = 10^{-1}$
$R_{Kz} = 0.50$
$R_{Kz} = 1.00$

a)

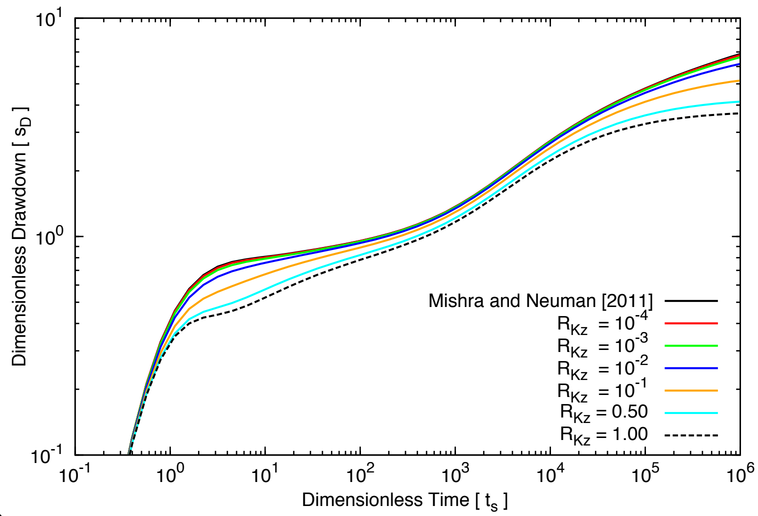
Dimensionless Drawdown [s_D]
Dimensionless Time [t_s]
10^{-1}
10^{0}
10^{1}
10^{2}
10^{3}
10^{4}
10^{5}
10^{6}
Mishra and Neuman [2011]
$R_{Kz} = 10^{-4}$
$R_{Kz} = 10^{-3}$
$R_{Kz} = 10^{-2}$
$R_{Kz} = 10^{-1}$
$R_{Kz} = 0.50$
$R_{Kz} = 1.00$

b)

Figure 3

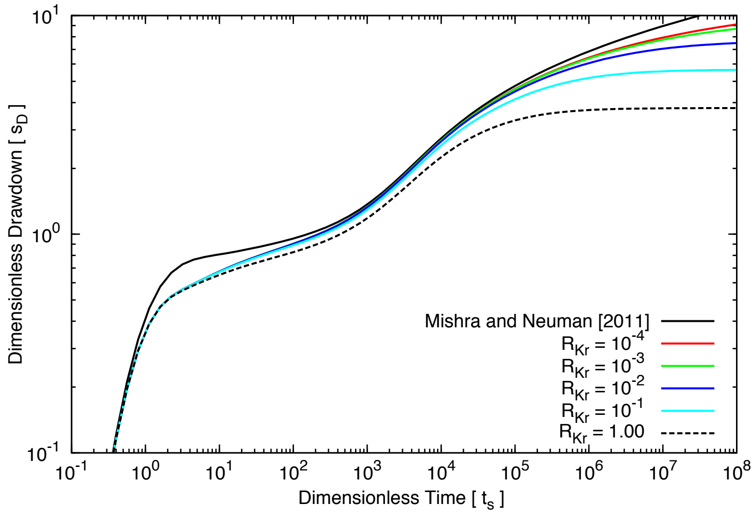

Figure 4

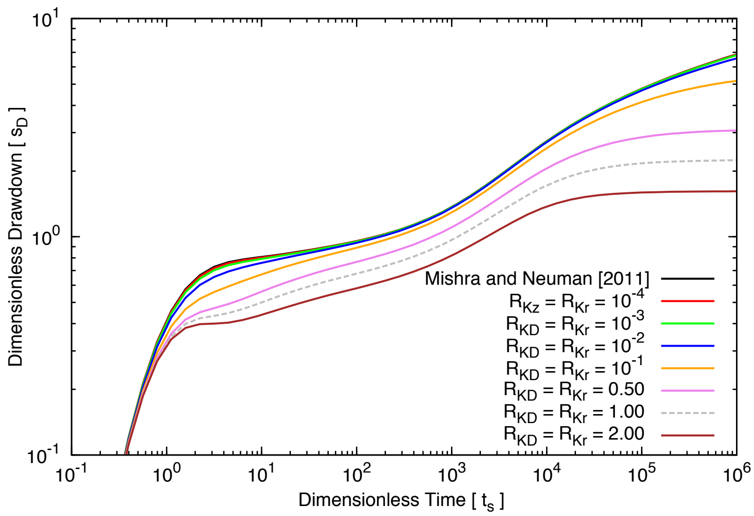

Figure 5

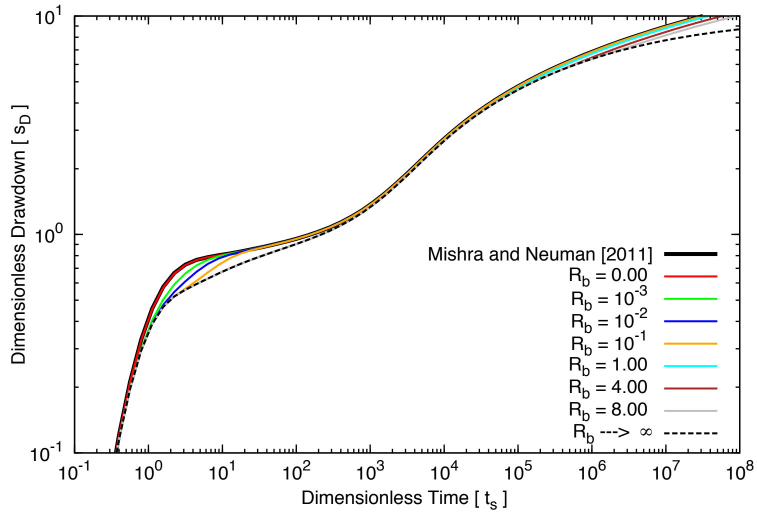

Figure 6

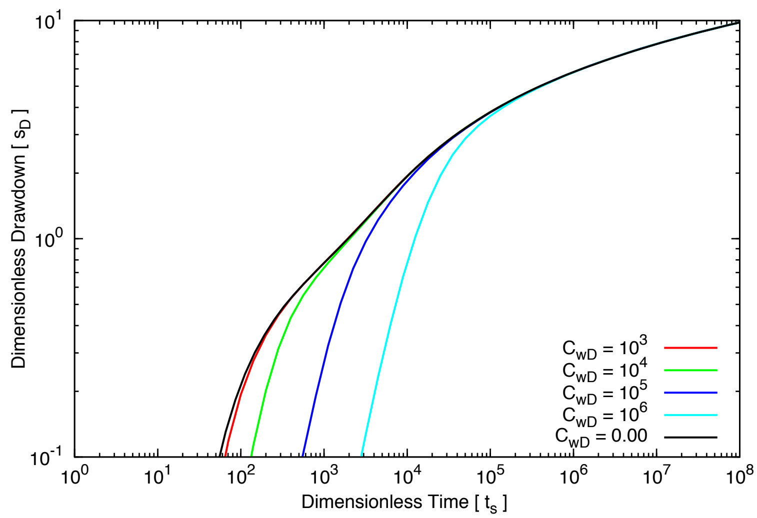

Figure 7

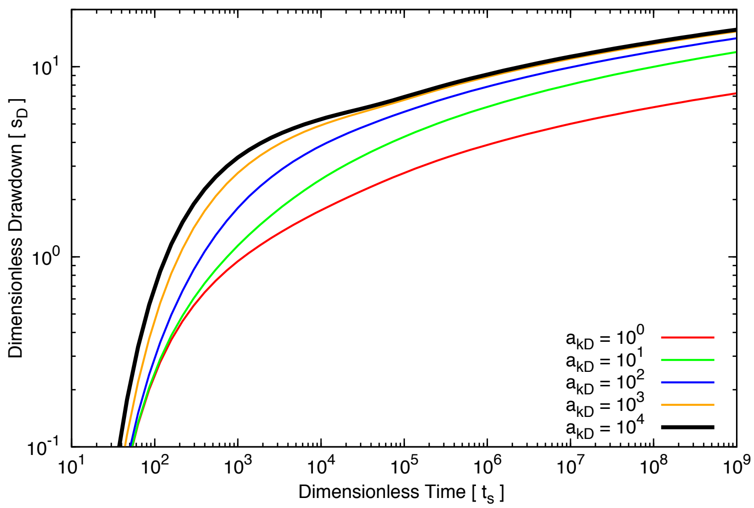

Figure 8

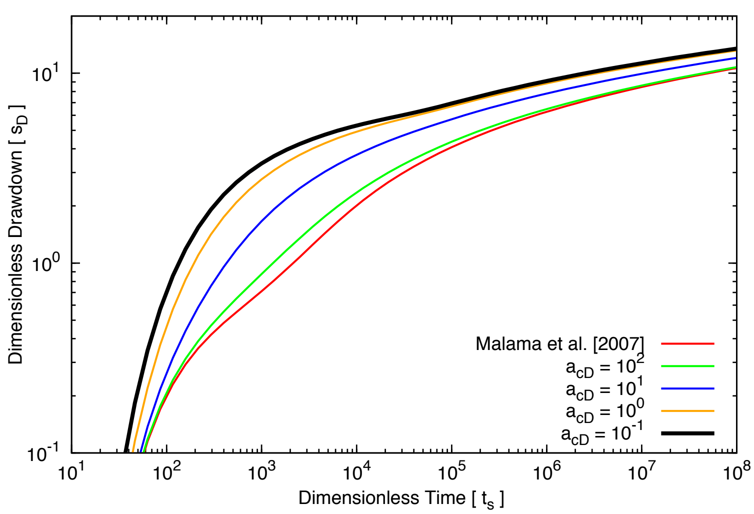

Figure 9